

SCIENTIFIC REPORTS



OPEN

RON4_{L1} is a new member of the moving junction complex in *Toxoplasma gondii*

Amandine Guérin¹, Hiba El Hajj², Diana Penarete-Vargas¹, Sébastien Besteiro¹ & Maryse Lebrun¹ 

Apicomplexa parasites, including *Toxoplasma* and *Plasmodium* species, possess a unique invasion mechanism that involves a tight apposition between the parasite and the host plasma membranes, called “moving junction” (MJ). The MJ is formed by the assembly of the microneme protein AMA1, exposed at the surface of the parasite, and the parasite rhoptry neck (RON) protein RON2, exposed at the surface of the host cell. In the host cell, RON2 is associated with three additional parasite RON proteins, RON4, RON5 and RON8. Here we describe RON4_{L1}, an additional member of the MJ complex in *Toxoplasma*. RON4_{L1} displays some sequence similarity with RON4 and is cleaved at the C-terminal end before reaching the rhoptry neck. Upon secretion during invasion, RON4_{L1} is associated with MJ and targeted to the cytosolic face of the host membrane. We generated a RON4_{L1} knock-out cell line and showed that it is not essential for the lytic cycle *in vitro*, although mutant parasites kill mice less efficiently. Similarly to RON8, RON4_{L1} is a coccidian-specific protein and its traffic to the MJ is not affected in absence of RON2, RON4 and RON5, suggesting the co-existence of independent MJ complexes in tachyzoite of *Toxoplasma*.

Apicomplexa parasites are responsible for important human and animal diseases. The phylum includes significant human pathogens such as *Plasmodium* species responsible for malaria, or *Toxoplasma* the agent of toxoplasmosis. The invasion process is a crucial step for these obligatory intracellular parasites and is mostly conserved throughout the phylum. In most cases, it involves the formation of a unique feature called Moving Junction (MJ). The MJ is a tight apposition between the host cell and parasite plasma membranes. This structure has been first observed in 1978 by electron-microscopy of *Plasmodium knowlesi* merozoites entering red blood cells¹, then its molecular characterization started being unraveled in *Toxoplasma* tachyzoites (the invasive form of the parasite responsible for the acute phase of the disease) almost 30 years later^{2,3}. The molecular components of the MJ are Apicomplexa-specific proteins^{2–5} secreted from two distinct apical organelles of the parasite called micronemes and rhoptries, the latter exhibiting a peculiar club-shape structure with a thin duct (or neck) and a bulbous part⁶. During invasion, the parasite translocates a microneme protein, the apical membrane antigen 1 (AMA1), at its own plasma membrane⁷, and exports a rhoptry neck complex (composed of RON2, RON4, RON5 and RON8 proteins) into the host cell⁴. It should be noted that RON8 is not universally conserved, but seems specific to coccidian parasites such as *Toxoplasma*, *Eimeria* and *Neospora*⁵. RON2 is inserted into the host plasma membrane and exposes a short segment at the surface of the host cell which interacts with AMA1^{8,9}. AMA1 and RON2 thus form an intimate contact^{10,11} which generates a close and irreversible interaction between the parasite and the host cell¹².

RON4, RON5 and RON8 are soluble proteins, tethered to RON2 and exposed to the cytosolic face of the host cell membrane⁴ where RON2, RON4 and RON5 cooperatively recruit host adaptor proteins that might contribute to anchor the parasite to the host cytoskeleton¹³. Parasites lacking RON4¹⁴ or RON8¹⁵ are viable but severely impaired in invasion. In contrast, it has not been possible to generate knock-out mutants for RON2¹² and RON5¹⁶, indicating a more critical role during invasion for those proteins. Conditional knock-down (KD) mutants for RON2 and RON5 exhibit an invasion defect of around 90%^{12,16}, while KO-RON4 and KO RON8 exhibit 60% and 70% reduction of invasion, respectively. In absence of RON8, the remaining MJ components RON2/RON4/RON5 are correctly targeted to the rhoptries and to the MJ, but 20% of parasites leave trails connecting the PVM with the

¹UMR 5235 CNRS, Université de Montpellier, 34095, Montpellier, France. ²Department of Internal Medicine and Experimental Pathology, Immunology and Microbiology, American University of Beirut, Beirut, 1107 2020, Lebanon. Correspondence and requests for materials should be addressed to M.L. (email: mylebrun@univ-montp2.fr)

host cell plasma membrane after invasion¹⁵. This suggests that RON8 could be required for an efficient fission of the PVM at the end of invasion. In contrast, RON2, RON4 or RON5 depletion induces expression and targeting defects of other members of the MJ complex, resulting in fact in triple functional mutants, hence limiting the phenotypic resolution of individual RON functions^{12–14,16}. In KD-RON2, KD-RON5 and KO-RON4 parasites, RON8 correctly localizes to the rhoptries and is found associated with the MJ during invasion in successful invaders^{12,13,16}. This indicates that an alternate MJ complex might be formed in absence of RON2, RON4 and RON5 in *Toxoplasma* tachyzoites, also possibly containing additional components. Recent studies showed that a MJ can also be formed in absence of AMA1 in tachyzoites^{12,17,18}. Deciphering the architecture of the MJ in complete absence of AMA1 has shown that tachyzoites knock-out for AMA1 upregulate homologs of AMA1 and RON2 that cooperate to support residual invasion^{12,19}. Not only this highlighted a likely functional redundancy in MJ components, but it also suggested some variety in MJ proteins, hinting that additional components remained to be discovered. RON4, unlike RON5 and RON8, possesses a putative homolog coded by a gene which was previously named *RON4_{L1}*²⁰ (www.Toxodb.org accession number TGGT1_253370). This gene displays a transcription profile that peaks during the S/M phase, a common characteristic of genes coding for rhoptry proteins²¹. Apart from transcriptional evidence for the *RON4L1* gene^{22,23}, nothing was known about the actual localization or role of the corresponding protein in the parasite.

In this report, we further investigate the molecular composition of the MJ complex by characterizing a new rhoptry neck protein, *RON4_{L1}*, that shares sequence homology with RON4 and is highly expressed in tachyzoites. We show that *RON4_{L1}* is a new member of the MJ complex that is present at the MJ and exposed at the cytosolic face of the host membrane during invasion. We successfully generated a direct knock-out of the *RON4_{L1}* gene. *RON4_{L1}*-depleted parasites invade cells similarly as control *in vitro* but are significantly impaired in virulence in mice, a defect restored by complementation with an additional *RON4_{L1}* copy. When RON4, RON2 and RON5 are down-regulated, *RON4_{L1}* expression and its localization in the neck of the rhoptry in intracellular parasites, or at the MJ during invasion, are unchanged. A characteristic ring shape labelling of RON8 and *RON4_{L1}* is observed in remaining invaders, supporting the existence of an alternate, coccidian-specific, complex for invasion independent of the main and more conserved among Apicomplexa RON2/RON4/RON5 complex. Taken together, our results offer a better understanding of the MJ architecture and support the existence of functional and independent MJ complexes in tachyzoites of *T. gondii*.

Results

RON4_{L1} is a new rhoptry neck protein. Transcriptomic and proteomic datasets in ToxoDB indicate that *RON4_{L1}* is expressed in tachyzoite, bradyzoite and sporozoite stages, as well as in the cat enteroepithelial stage (www.Toxodb.org). Like RON8, *RON4_{L1}* is a coccidian-specific protein. *RON4_{L1}* shows 13% identity and 21% similarity with RON4 (Fig. S1): *RON4_{L1}* is noticeably longer than RON4, and essentially homologous to its C-terminal region. *RON4_{L1}* is a 1981 amino acids long protein, with a predicted molecular mass of 216 kDa. Besides a predicted signal peptide, no transmembrane domain or any other known recognized domains can be identified.

To localize *RON4_{L1}*, we first tagged the protein with a triple hemagglutinin tag (HA₃) at the C-terminal end, by single recombination at the endogenous locus, as described previously²⁴ and represented in Fig. 1a. A clone was selected and verified by PCR for proper construct integration (Fig. 1b). IFA using anti-HA antibodies revealed that only a fraction of the parasites display a HA₃-tag signal, although when present, the signal observed was reminiscent of the pre-rhoptry compartments of developing parasites (data not shown). Because many rhoptry proteins are processed in the secretory pathway in the transition step between immature (pre-rhoptry) and the mature organelle, this labelling suggested that *RON4_{L1}* is a rhoptry protein potentially undergoing a C-terminal proteolytic maturation. To verify this hypothesis, we first performed co-localization with the pre-rhoptry marker Pro-ROP4²⁵. When tagged at its C-terminal-end, *RON4_{L1}* co-localizes perfectly with the immature ROP4 protein stored in the pre-rhoptries (Fig. 1c, upper panel), while it is absent of mature organelles detected with anti-RON2 antibodies (Fig. 1c, lower panel). This indicated that *RON4_{L1}* likely travels through the secretory pathway, is addressed to the pre-rhoptries and undergoes a C-terminal cleavage during trafficking to mature organelles. To confirm this hypothesis, we then added a tag at the N-terminus part of the protein in order to follow the mature protein. A strategy was designed to insert a HA₃-tag after the signal peptide of *RON4_{L1}* in the $\Delta ku80$ RH strain by CRISPR/Cas9-mediated genome editing (Fig. 2a) using a specific donor sequence (Fig. S2) as a template for homologous recombination. Transfected parasites were sorted by FACS to enrich the Cas9-YFP transfected population and then cloned immediately. PCR amplifications (Fig. 2b) and sequencing confirmed the insertion of the HA₃ tag after the signal peptide of *RON4_{L1}* in a clone referred hereafter as HA₃-*RON4_{L1}*, by opposition to the C-terminal tagged *RON4_{L1}*-HA₃ strain. HA labelling of HA₃-*RON4_{L1}* parasites delineated the pre-rhoptries in some parasites, as observed for *RON4_{L1}*-HA₃ parasites (Fig. 2c upper panel). However, in contrast to the C-terminal tagging, the remaining HA₃-*RON4_{L1}* parasites displayed an apical labeling that co-localized perfectly with the rhoptry neck marker RON2 (Fig. 2c lower panel).

Western blot analysis with anti-HA antibody showed that a faint high molecular weight product was observed in protein extracts from the C-terminus tagged cell line, likely corresponding to the unprocessed form (Fig. 2d). While this form was also detected in lysates from the N-terminus tagged cell line, the main product had a lower molecular mass (Fig. 2d). Several lower bands, possibly corresponding to further processing or degradation products, were also detected (Fig. 2d).

In conclusion, *RON4_{L1}* is a new rhoptry neck protein that undergoes a C-terminal cleavage during rhoptry maturation (Fig. 2e).

RON4_{L1} is a new component of the MJ RON complex exposed to the cytosolic face of the host cell during invasion. In order to know if *RON4_{L1}* is secreted during invasion, we performed IFAs on

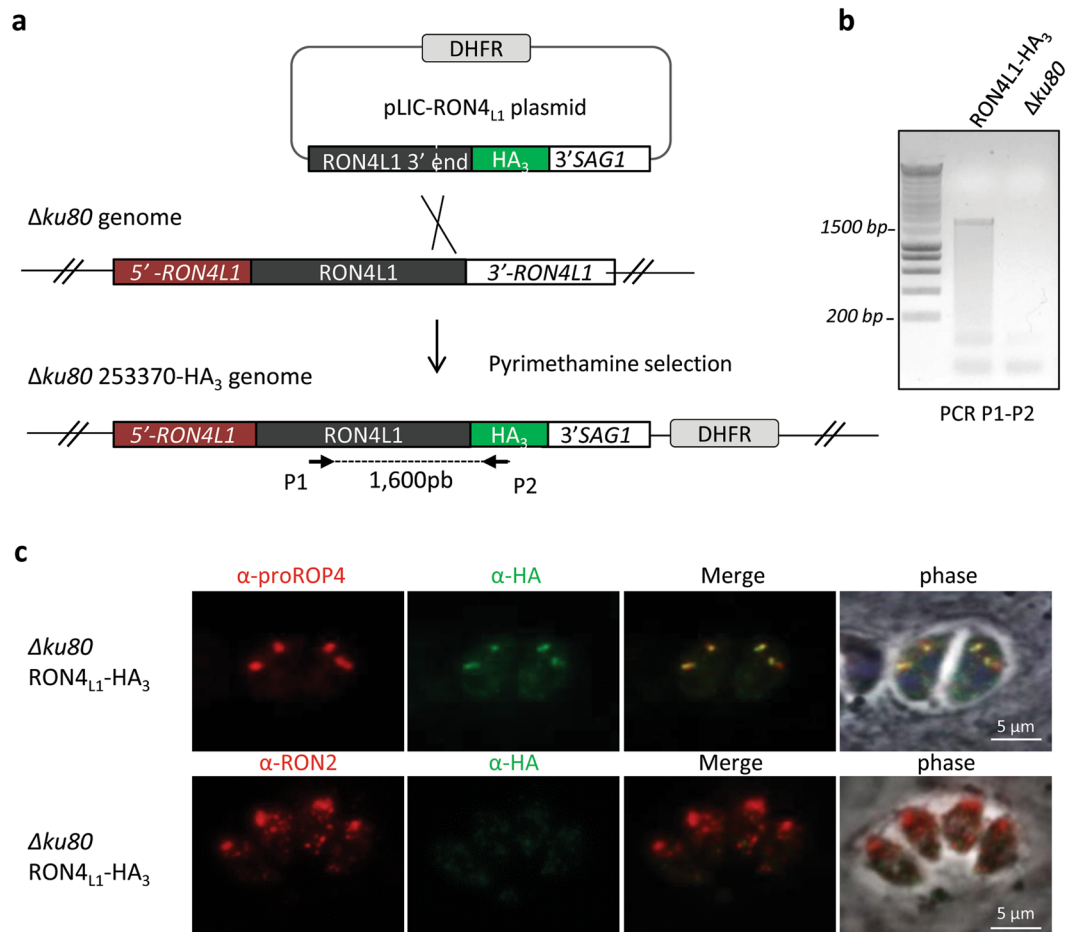


Figure 1. Epitope tagging of RON_{4L1}. (a) Scheme illustrating the approach used to endogenously tag RON_{4L1} at the C-terminus. Primers used to verify the genetic modification and the size of the PCR product are indicated. (b) The HA₃ tagging at the 3' end of RON_{4L1} locus by single homologous recombination was verified with PCR using primers P1 and P2, whose positions are indicated in (a). (c) IFA on intracellular $\Delta ku80$ RON_{4L1}-HA₃ parasites using anti-pro-ROP4 and anti-HA antibodies (upper panel) or anti-RON2-4 antibodies (lower panel). The anti-HA antibodies stains only the pre-rhoptries. Scale bars, 5 μ m.

HA₃-RON_{4L1} parasites using anti-HA antibodies, with permeabilization conditions optimized to detect only the material secreted by the parasite²⁶. Indeed, with low saponin concentration, rhoptries membranes are not permeabilized, and antibodies detect the protein only once secreted from the organelle. On invading parasites, the RON_{4L1} labelling was circumferential, coincided with the constriction of the parasite, and co-localized with the MJ marker RON2 (Fig. 3a, panels 1 and 2). After complete internalization, RON_{4L1} co-localized with RON2 as a puncta systematically observed at the posterior end of the parasite, which corresponds to the residual MJ (Fig. 3a, panel 3). Overall, our results indicate that RON_{4L1} is part of the MJ.

To test whether RON_{4L1} physically interacts with the RON2/RON4/RON5/RON8 MJ complex, we performed an immunoprecipitation using anti-HA beads on a HA₃-RON_{4L1} parasites lysate. All components of the MJ complex (RON2, RON4, RON5, RON8 and AMA1) were co-immunoprecipitated together with RON_{4L1}, even in stringent experimental conditions (1 M NaCl washes) (Fig. 3b), suggesting a strong interaction.

Finally, we sought to test the topology of RON_{4L1} at the MJ. We were unable to identify any putative transmembrane domains in RON_{4L1} using prediction software such as TMHMM (<http://www.cbs.dtu.dk/services/TMHMM>) or PredictProtein (<https://www.predictprotein.org>). We thus suspected the protein might be associated with RON4, RON5 and RON8 on the cytoplasmic side of the host cell. To test this possibility, we used the “glass-bead loading” approach previously described to demonstrate the export of RONs and their association with the cytosolic face of the host membrane⁴. The design of this experiment, based on cytoplasmic loading of antibodies within the host cell prior to invasion, allows the detection of RON_{4L1} at the MJ only if the protein is secreted into the host cell cytoplasm (see Methods). This is illustrated by the left panel of Fig. 3c, in which one parasite is extracellular (SAG1 positive, right), while the second is intracellular (SAG1 negative, left) and the latter is also stained with RON_{4L1}. This characteristic signal corresponding to the residual MJ shows that RON_{4L1} is exposed on the cytoplasmic side of the host cell. In the same experimental conditions, for invading parasites (Fig. 3c, right panel) RON_{4L1} was also detected at the ring-like MJ.

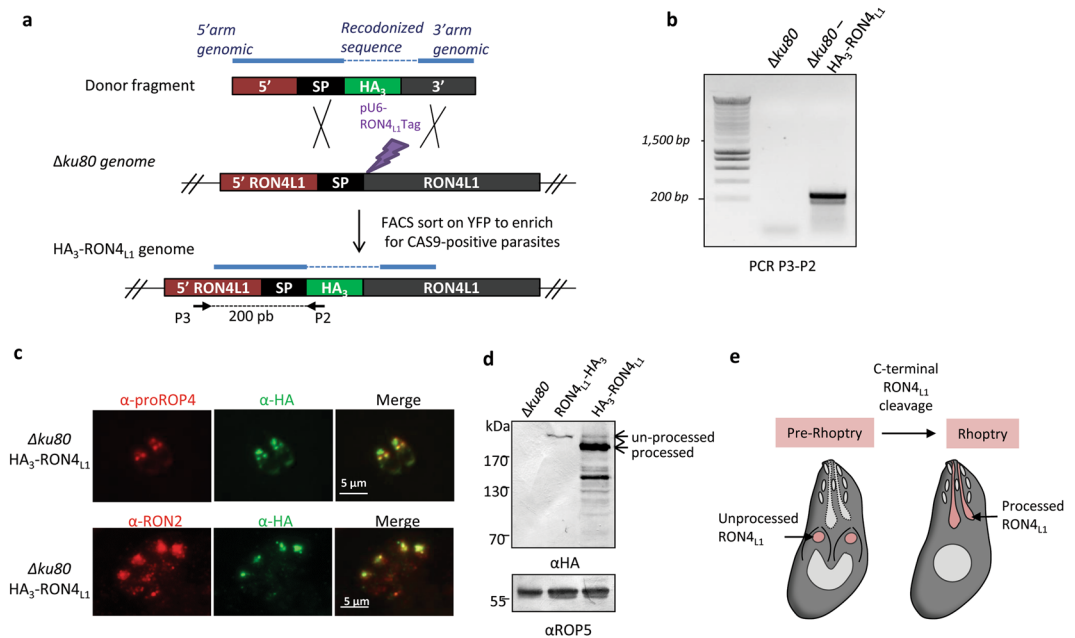


Figure 2. RON4_{L1} is a new rhoptry neck protein, cleaved at the C-terminal end. **(a)** Scheme illustrating the approach used to endogenously tag RON4_{L1} at the N-terminus end in *Δku80* using CRISPR/Cas9 nuclease mediated gene recombination strategy. To induce a double strand break just downstream the sequence signal of RON4_{L1} (black) and introduce a HA₃-tag by double homologous recombination, a cas9-yfp-RON4_{L1} gRNA expression plasmid (pU6- RON4_{L1} Tag) was transfected together with a linear 442 bp donor DNA fragment containing RON4_{L1} homology regions for double strand break repair. YFP-positive parasites were sorted by FACS to enrich for Cas9-expressing parasites. Recodnized DNA sequence of the donor fragment is hatched. Primers used to verify the genetic modification and the size of the PCR product are indicated. **(b)** The HA₃ tagging at the 5' end of the coding sequence of RON4_{L1} locus by double homologous recombination was verified with PCR using primers P3 and P2. **(c)** IFA on intracellular *Δku80* HA₃-RON4_{L1} parasites using anti-proROP4 and anti-HA antibodies (upper panel) or anti-RON2-4 antibodies (lower panel). The anti-HA antibody stains the pre-rhoptries and the neck of the rhoptry of HA₃-RON4_{L1} parasites. Scale bars, 5 μm. **(d)** Western blot of *Δku80*, RON4_{L1}-HA₃ and HA₃-RON4_{L1} strains using anti-HA antibodies. ROP5, loading control. **(e)** Scheme illustrating (on the left) a parasite during endodyogeny process (S/M phase) with immature pre-rhoptries (pink) and (on the right) a parasite in S phase with mature rhoptries. The unprocessed form of RON4_{L1} is present in immature rhoptries while the C-terminal cleaved RON4_{L1} is present in mature rhoptries. Full-length blots/gels are presented in Fig. S6.

From these experiments, we conclude that RON4_{L1} is a new member of the MJ complex that is exposed on the cytoplasmic face of the host cell, together with RON2, RON4, RON5 and RON8 (Fig. 3d).

RON4_{L1} is correctly targeted to the neck of the rhoptry in KD-RON4 and remains associated with the MJ on invading parasites. In KD-RON2, KD-RON4 and KD-RON5 mutants, the formation of the RON2/RON4/RON5 complex is disrupted^{12,13,16}, while RON8 is expressed in normal amount and traffics correctly to the MJ. We thus sought to investigate the fate of RON4_{L1} in a parasite where the formation of the RON2/RON4/RON5 complex is affected. To this end, we introduced a triple HA epitope-tag after the signal sequence of RON4_{L1} in the KD-RON4 background (Fig. S3), using the same strategy as described in Fig. 2a. As previously observed, altering RON4 expression leads to a significant decrease of RON2 and RON5 expression (Fig. 4a). In contrast, and similarly to RON8, RON4_{L1} is expressed at normal levels (Fig. 4a) and correctly associated with rhoptries in intracellular parasites (Fig. 4b) and at the MJ in invading parasites (Fig. 4c). In conclusion, similarly to RON8, RON4_{L1} traffic seems independent of RON2, RON5 and RON4 proteins expression and complex formation.

RON4_{L1} plays a role in virulence in a mouse model. To test the function of RON4_{L1}, we used a CRISPR/Cas9 strategy to generate a knock-out cell line by replacing a 22.2 kbp genomic region encompassing the RON4_{L1} open reading frame by a *DHFR* cassette in the HA₃-RON4_{L1} cell line background (Fig. 5a). Knock-out parasites (KO-RON4_{L1}) were obtained, as verified by diagnostic PCR (Fig. 5b), western blot (Fig. 5c) and IFA (Fig. 5d and Supplementary Fig. S4). This demonstrates RON4_{L1} is not required for parasite survival *in vitro*. While RON4_{L1} is not detected at the MJ of KO-RON4_{L1} parasites, remaining members of the RON complex (RON2, RON4, RON5 and RON8) are still expressed at normal levels (Fig. 5e). The localization of these proteins also remains unaltered: they are present in the neck of the rhoptries in intracellular parasites (Fig. S4) and at the MJ during invasion (Fig. 5d).

To test the consequence of the loss of RON4_{L1} on the parasite lytic cycle, we then performed a plaque assay, and found that the size of lysis plaques was similar between wild-type and KO-RON4_{L1} parasites (Fig. 6a). Besides,

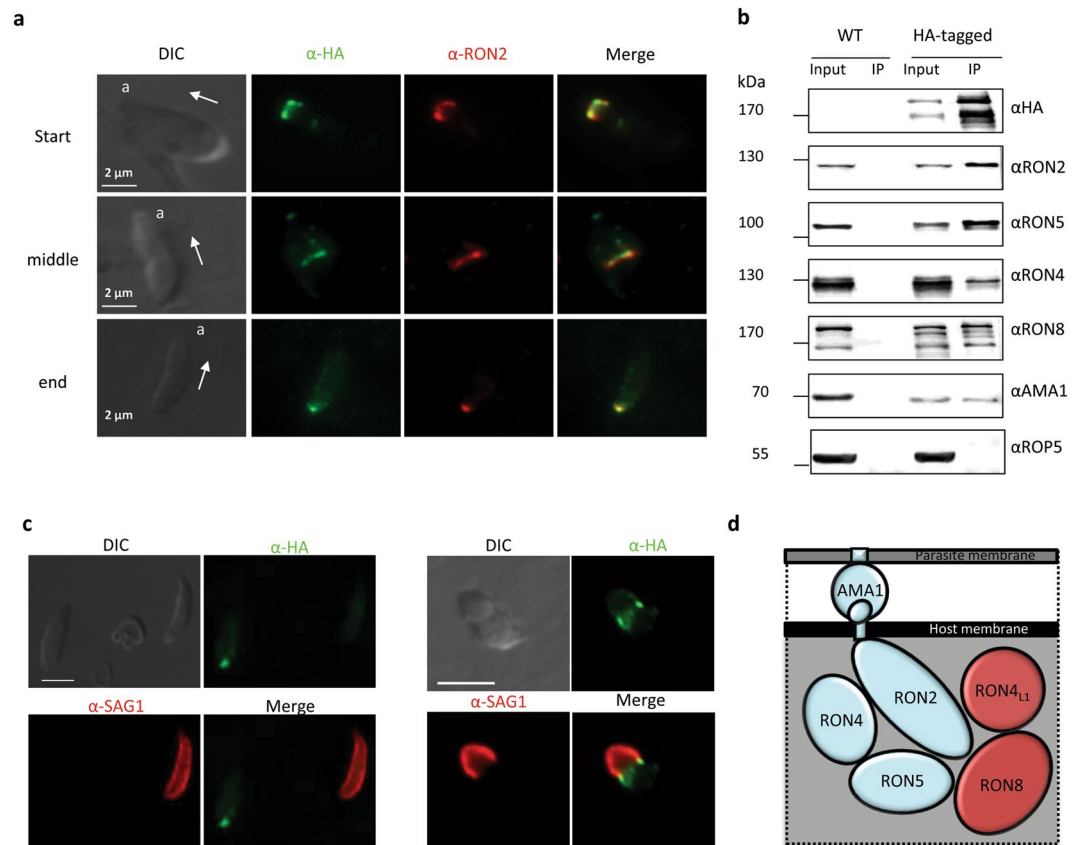


Figure 3. RON_{4L1} is part of the MJ complex AMA1/RON2/RON4/RON5/RON8 and associated with the host cytosolic face of the MJ during invasion. **(a)** IFA on invading $\Delta ku80$ HA₃-RON_{4L1} strain using anti-HA and anti-RON2-4 antibodies. The first two panels illustrate parasites at the beginning and half way of the invasion process. Panel 3 illustrates the staining of RON_{4L1} and RON2 when invasion is complete. RON_{4L1} is detected associated with the MJ in $\Delta ku80$ HA₃-RON_{4L1} parasites. Arrows indicate the direction of motion. a, apical end. Scale bar, 2 μ m. DIC: differential interference contrast. **(b)** Co-immunoprecipitation using anti-HA antibodies on $\Delta ku80$ HA₃-RON_{4L1} parasites, followed by an immunoblot using rabbit anti-RON2-3, rat anti-RON8, rabbit anti-RON4, rat anti-RON5, rabbit anti-AMA1 and rat anti-HA antibodies reveals the association of RON_{4L1} with the MJ complex. ROP5, negative control. Full-length blots are presented in Fig. S6. **(c)** Glass beads pre-loading of host cells with anti-HA antibodies to follow the topology of RON_{4L1} at the MJ. Cells were loaded by antibodies directed against HA epitope as described in Materials and Methods and were pulse-infected for 2 min 30 s with $\Delta ku80$ HA₃-RON_{4L1} parasites. The extracellular portion of the tachyzoite was labelled with anti-SAG1 (red), and, then, after permeabilization of the cells with saponin, the host cell-exposed part of the MJ was revealed by addition of the conjugate antibody (green). Image on the left panel shows one parasite intracellular (labelled with anti-SAG1 antibodies). Image on the right panel shows a parasite in the process of invasion with only half extracellular (red) with the ring of the RON_{4L1} at the MJ (labelled with anti-HA antibodies, green). Scale bar, 5 μ m. DIC: differential interference contrast. **(d)** Schematic representation of the current model of MJ complex organization, now including RON_{4L1}. AMA1, exposed at the surface of the parasite, interacts with a short portion of RON2, while the rest of the RON2, together with RON4, RON5, RON8 and RON_{4L1} are exposed in the cytosol of the host cell. Conserved RONs proteins in Apicomplexa are in blue, while Coccidian RON8 and RON_{4L1} are in red. Note that the stoichiometry of the complex at the MJ is currently unknown.

no apparent defect of invasion was detected in fibroblastic cells (Fig. 6b). We next assessed if the loss of RON_{4L1} could impact parasite virulence in the mouse model (Fig. 6c). The mortality of mice infected with KO-RON_{4L1} was delayed (4 to 5 days) compared with that of mice infected with parasites of $\Delta ku80$ parental strain or with a cosmid-complemented RON_{4L1}-reexpressing cell line (Cpt-RON_{4L1}) (Supplementary Fig. S4). These results show that even if the loss of RON_{4L1} is not significantly impacting *in vitro* growth, the protein contributes to parasite virulence *in vivo*.

Discussion

The formation of the MJ is an essential mechanism for many Apicomplexan parasites including *Plasmodium* and *Toxoplasma* species. In *Toxoplasma*, the parasite MJ components are composed of AMA1, a micronemal protein exposed on the surface of the parasite, and of a complex of rhoptry neck proteins comprising RON2, RON4,

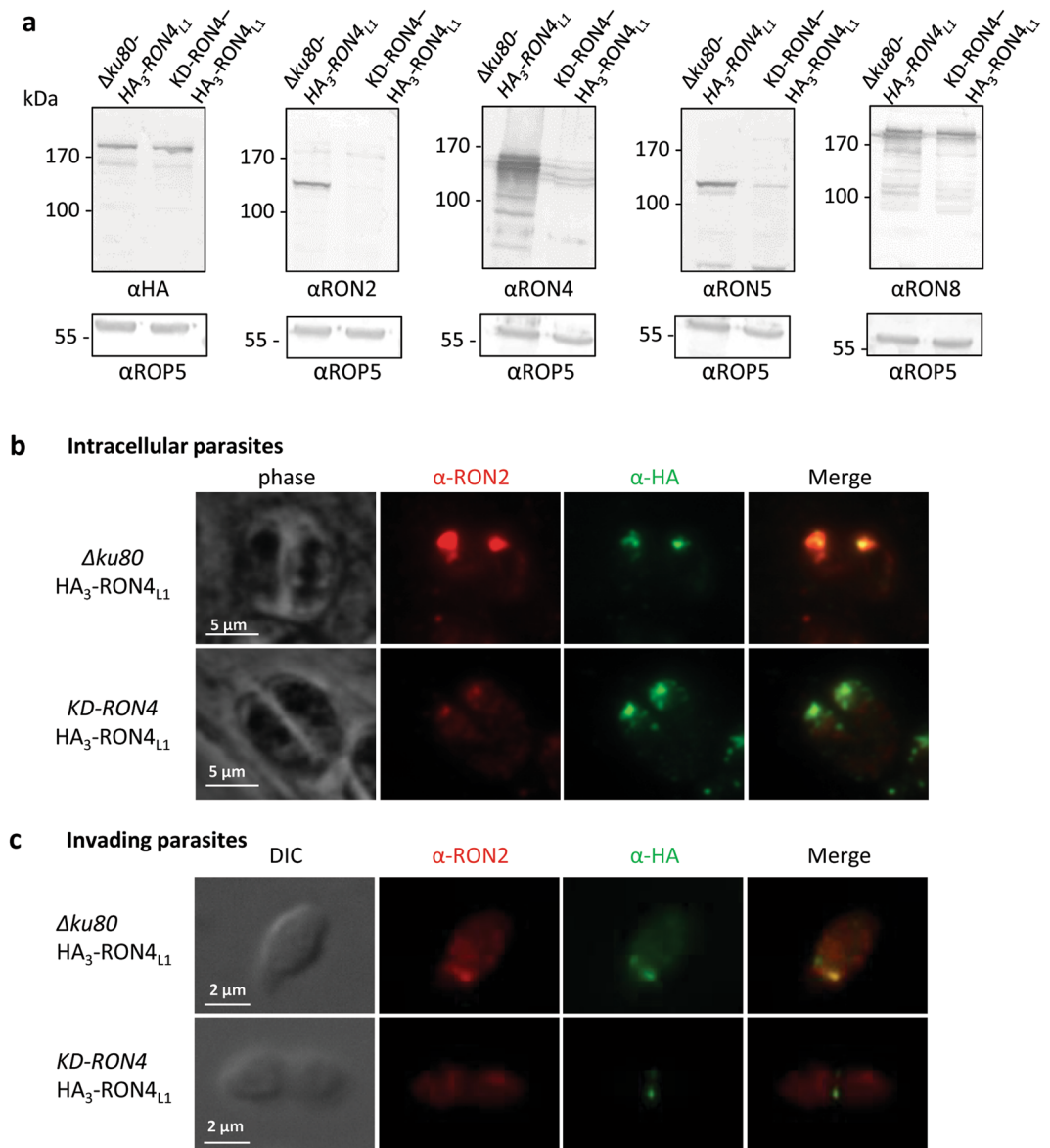


Figure 4. RON4_{L1} expression and localization is independent of the RON2/4/5 complex. **(a)** Western blot analysis of $\Delta ku80$ HA₃-RON4_{L1} and KD-RON4 HA₃-RON4_{L1} parasite lysates treated with ATc for 48 hours using anti-HA, anti-RON2-3, anti-RON4 rabbit, anti-RON5 and anti-RON8 antibodies. RON4_{L1} expression is not affected by RON2, RON4 and RON5 depletion. ROP5: loading control. Full-length blots are presented in Supplementary Fig. 6. **(b)** IFA of intracellular KD-RON4 parasites in which RON4_{L1} has been HA₃-tagged. RON4_{L1} localizes in the neck of the rhoptries, as shown by the co-localization with RON2. Scale bar, 2 μ m. **(c)** IFA of invading KD-RON4 HA₃-RON4_{L1} parasites. RON4_{L1} remains present at the moving junction in invading KD-RON4 parasites. Scale bar, 2 μ m. DIC: differential interference contrast.

RON5 and RON8. In the present study, we identify a new rhoptry neck protein, RON4_{L1}, associated with the MJ complex. RON4_{L1} has been identified through its partial homology with the RON4 protein. In contrast to the paralogs of RON2, RON2_{L1} and RON2_{L2} which are preferentially expressed in sporozoites or bradyzoites, and up-regulated upon depletion of AMA1^{12,19,27}, RON4_{L1} is abundant in tachyzoites and is not up-regulated in the KD-RON4 mutant. Thus, RON4_{L1} is a constitutive component of the MJ complex in tachyzoites.

While RON2, RON4 and RON5 are conserved in most Apicomplexa, RON8 and RON4_{L1} are specific to *Coccidia*. Little is known about how RON proteins traffic to the rhoptry neck. RON5 is believed to be important for RON2 stability and RON4 targeting¹⁶. Similarly, RON2 and RON4 also play a role in stabilizing the RON2/RON4/RON5 complex^{8,13,14}. Thus, depletion of either RON2, RON4 or RON5 is sufficient to reduce the expression and localization of the others. In contrast, their depletion does not influence the behavior of the coccidian-specific MJ members RON8^{8,13,16} and RON4_{L1} (this study). Homologs of RON2 and RON4 and RON5 can be found in many Apicomplexa parasites, supporting the idea of a conserved RON2/RON4/RON5 core complex, and the existence of additional members which would be species specific. Both RON8 and RON4_{L1} are

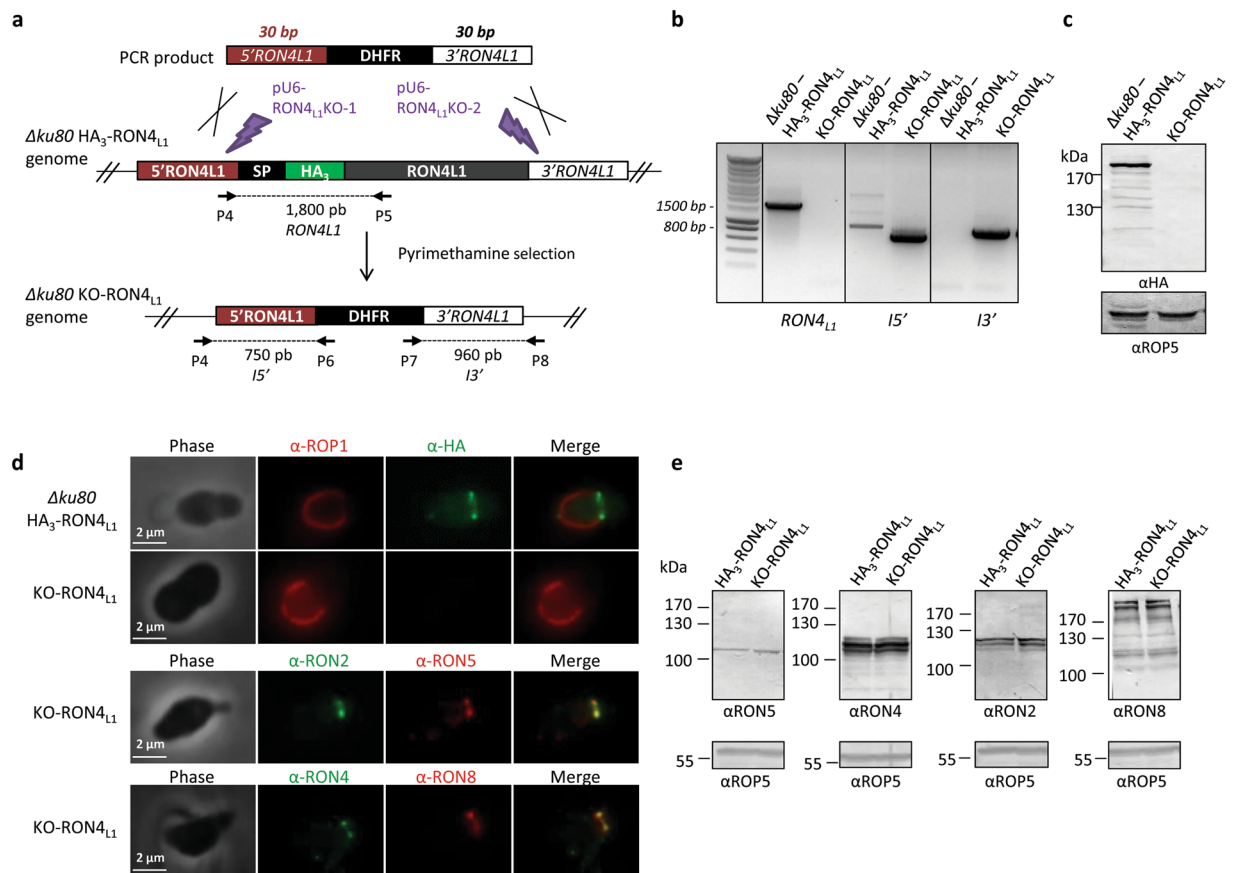


Figure 5. Deletion of $RON4_{L1}$ does not affect the expression and localization of the $RON2/RON4/RON5/RON8$ complex. (a) Scheme representing the approach used to generate a straight knock-out for $RON4_{L1}$ in $\Delta ku80$ HA_3-RON4_{L1} strain. Two protospacers (pU6- $RON4_{L1}$ KO-1 and -2; in purple) were designed to induce a double strand break in the 5'UTR and 3'UTR of the $RON4_{L1}$ gene. A PCR amplifying the DHFR cassette flanked with 30 bp homology sequences of the 5' and 3'UTR of $RON4_{L1}$ was used as a donor DNA fragment for DNA repair, inducing the removal of the entire $RON4_{L1}$ gene. Primers used to amplify $RON4_{L1}$, I3' and I5' fragments and the sizes of the PCR products are indicated. (b) PCR verification of DHFR integration at $RON4_{L1}$ locus. (c) Western blot using anti-HA antibodies shows the depletion of $RON4_{L1}$ in the KO- $RON4_{L1}$ strain. ROP5: loading control. (d) IFA on invading KO- $RON4_{L1}$ parasites using anti-ROP1, anti-HA, anti- $RON2-4$, anti- $RON5$, anti- $RON4$ and anti- $RON8$ antibodies. $RON4_{L1}$ labelling is lost in KO- $RON4_{L1}$ parasites while the others members of the RON complex are still present at the MJ. Scale bar, 2 μm . (e) Western blots analysis using anti- $RON2-3$, anti- $RON5$, anti- $RON8$ and rabbit anti- $RON4$ antibodies on HA_3-RON4_{L1} parental line and KO- $RON4_{L1}$ mutant reveal normal expression of $RON2$, $RON4$, $RON5$ and $RON8$. Full-length blots and gels are presented in Supplementary Fig. 6.

soluble proteins exposed to the cytosolic face of the MJ (Fig. 3d). How they associate with the MJ during the progression of invasion in the absence of the core complex remains unknown. This is particularly intriguing, because so far $RON2$ is the only known membrane anchor for the RON complex in tachyzoites: it is inserted as a transmembrane protein into the host cell surface, and is supposed to serve as a host connector (via AMA1) to the gliding machinery necessary for the progression of internalization²⁸. The localization of both $RON8$ and $RON4_{L1}$ to a MJ-like ring during invasion in absence of $RON2$ suggests additional $RONs$ might compensate the anchoring function. Whether $RON2_{L1}$, which is normally expressed at very low level in tachyzoite, could be such a candidate, needs further investigations.

While $RON2$ and $RON5$ are essential for tachyzoites^{12,16}, $RON8$ and $RON4$ are dispensable^{14,15}. Nevertheless, $RON8$ depletion led to a 70% reduction of invasion and a failure to close the PVM properly after successful invasion events. This invasion defect translates to radically impaired virulence in infected mice. Here we showed that $RON4_{L1}$ is also not essential *in vitro* and the absence of $RON4_{L1}$ had no visible impact on the formation of the MJ or the vacuole. Accordingly, the $RON4_{L1}$ knock-out parasites we generated were not affected in the lytic cycle and invaded fibroblast cells as efficiently as wild-type parasites. Nevertheless we cannot exclude a potential compensatory effect through the up-regulation of other(s) gene(s), as it has been observed for $RON2$ and AMA1¹². However, interestingly our *in vivo* experiments showed that in absence of $RON4_{L1}$, the parasites were less virulent. A delay of four to five days was observed compared to infection with parental parasites; this small but consistent delay was abolished by complementation with an exogenous $RON4_{L1}$ copy. It is not yet clear if the attenuation of

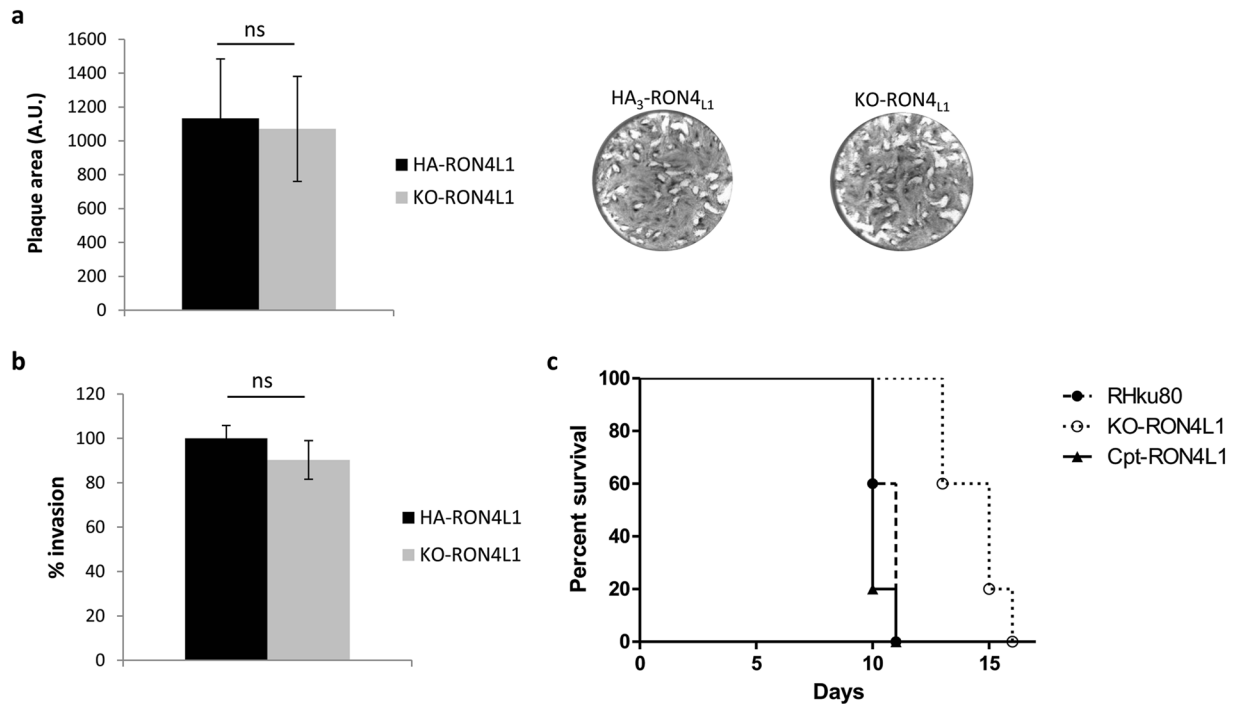


Figure 6. Phenotypic consequences of RON4_{L1} disruption. **(a)** Plaque assay of HA₃-RON4_{L1} and KO-RON4_{L1} parasites. Parasites were added on HFF monolayer for 7 days and the size of lysis plaques was measured. AU: arbitrary units. Values are the mean standard error of the mean plaque area (20 plaques were measured in each condition) from one representative experiment out of two. No defect of the lytic cycle has been observed in the KO-RON4_{L1} mutant using a two-tailed t-test. **(b)** Invasion assay for 5 minutes in HFF cells of HA₃-RON4_{L1} and KO-RON4_{L1} parasites. Values represent means \pm SD, $n = 3$, from a representative experiment out of 2 independent assays. No defect of invasion was observed *in vitro* for the KO-RON4_{L1} strain using a two-tailed t-test. **(c)** *In vivo* virulence of $\Delta ku80$, KO-RON4_{L1} and *cpt*-RON4_{L1} parasites in a mouse model. $n = 5$. Logrank tests show a significant difference between WT and KO-RON4_{L1} ($P = 0.031$) and between KO-RON4_{L1} and *Cpt*-RON4_{L1} ($P = 0.0016$), while no difference between WT and *Cpt*-RON4_{L1} was observed. Representative data out of 2 experiments.

virulence observed *in vivo* can be directly linked to a defect in invasion that was not discernible in our *in vitro* fibroblast assay. For instance, a specific role for RON4_{L1} during invasion of a peculiar cell type cannot be excluded. In the mouse model, slight alterations in parasite tropism, tissue migration, and invasion success rates can have potential greater consequences on parasite fitness. Transcriptomic and proteomic data sets in ToxoDB show that, in contrast to RON2, RON4, RON5 and RON8, RON4_{L1} is also expressed in the cat enteroepithelial stage. This could suggest also a role for RON4_{L1} in invasion of merozoites in the intestine.

In contrast to other Apicomplexa, Coccidia such as *Toxoplasma* and *Neospora* have very broad host specificity. The expression of additional RON proteins like RON8 and RON4_{L1} might illustrate an enriched MJ proteins repertoire in these parasites that would support their ability to invade a large variety of cell types.

Methods

Ethics statement. All animal work was conducted in strict accordance with the AAALAC (Association for Assessment and Accreditation of Laboratory Animal Care International) guidelines and the guide of animal care use book (Guide, NRC 2011). All mice protocols were approved by the Institutional Animal Care and Utilization Committee (IACUC) of the American University of Beirut (IACUC Permit Number IACUC#14-3-295). All animals were housed in specific pathogen-free facilities. Humane endpoints were used as requested by the AUB IACUC according to AAALAC (Association for Assessment and Accreditation of Laboratory Animal Care International) guidelines and guide of animal care use book (Guide, NRC 2011). Mice were sacrificed for any of the following reasons: 1) impaired mobility (the inability to reach food and water); 2) inability to remain upright; 3) clinical dehydration and/or prolonged decreased food intake; 4) weight loss of 15–20%; 5) self-mutilation; 6) lack of grooming behavior/rough/unkept hair coat for more than 48 hours; 7) significant abdominal distension; 8) unconsciousness with no response to external stimuli. Animals were deeply anesthetized before cervical dislocation. Eye pricks were done following deep anesthesia with isoflurane and all efforts were made to minimize suffering.

Parasite culture. All *T. gondii* tachyzoites were passaged in human foreskin fibroblasts (HFFs) (American Type Culture Collection-CRL 1634) or Vero cells (American Type culture Collection CCL 81) grown in Dulbecco's modified essential medium (Gibco-BRL), supplemented with 5% fetal calf serum and 2 mM glutamine. Tachyzoites of the *T. gondii* RH strain deleted for *ku80* gene ($\Delta ku80$)²⁴ were used throughout the study.

Cloning of DNA constructs. Excepted when notified, all PCR amplifications were performed with the Phusion polymerase (NEB Biolabs) and the primers are listed in Supplementary Table S1.

To tag RON_{4L1} at the C terminal end of $\Delta ku80$ parasites, we produced a pLIC-RON_{4L1} plasmid based on pLIC-DHFR-HA₃²⁴. The 3' end of RON_{4L1} gene was amplified with primers P11/P12, cloned in frame with the triple hemagglutinin tag in pLIC-DHFR-HA₃ vector and linearized by *Xho*I prior to transfection. Single homologous recombination at the endogenous locus allowed the endogenous tagging of RON_{4L1}.

To tag RON_{4L1} at the N terminal end just after the signal peptide, we used the CRISPR/Cas9 strategy. We designed a protospacer that would recruits Cas9 to cut 21 bases pairs downstream the end of the sequence signal codon and a donor DNA to insert triple HA by double homologous recombination. The sequence of the donor DNA is provided in Fig. S2. The protospacer sequence GACAATGCCGCCACGTGTGA was cloned by annealing primers P13 and P14 and cloning *Bsa*I site of vector pU6-Cas9-YFP (gift of B. Striepen, UGA). The resulting plasmid pU6-RON_{4L1}Tag contains a Cas9-YFP fusion allowing selection of fluorescent parasites by FACS. The template sequence containing the HA₃ sequence was generated by IDT services and TOPO-cloned. A 442 bases pairs PCR product corresponding to the template was amplified with KOD polymerase (Novagen) using primers P15/P16 and co-transfected with pU6-RON_{4L1}Tag in $\Delta ku80$ or KD-RON4 strains.

A CRISPR/Cas9 strategy was settled up to generate a knock-out of the gene RON_{4L1}. A fragment donor corresponding to the DHFR resistance cassette flanked by 30 bp homology arms of RON_{4L1} gene was amplified with KOD polymerase (Novagen) using primers P17 and P18. Two pU6-Cas9-YFP vectors were constructed. pU6-RON_{4L1}KO-1 plasmid contains a protospacer targeting 11 bp after the start codon and pU6-RON_{4L1}KO-2 plasmid targets 13 bp before the stop codon. pU6-RON_{4L1}KO-1 and 2 plasmids were generated by annealing primers P19 and P20 or P21 and P22, respectively. The PCR product corresponding to the donor fragment and the two pU6-RON_{4L1}KO plasmids were co-transfected in $\Delta ku80$ HA₃-RON_{4L1} strain allowing the removal of the entire RON_{4L1} gDNA of 22.2kbp.

Complementation of the KO-RON_{4L1} has been done through the integration of the cosmid PSBMF65 (ToxoDB), which encompasses the entire gDNA of RON_{4L1} and contains a bleomycin cassette for selection. It was randomly inserted into the genome. Clones were obtained after phleomycin selection.

Immunoblots. Proteins from freshly egressed tachyzoites were resuspended into SDS buffer, separated on 10% SDS PAGE and transferred to nitrocellulose membranes. Primary antibodies used are listed in Supplementary Table S2 and diluted in 5% non-fat dry milk in TNT buffer (140 mM NaCl, 15 mM Tris, 0.05% Tween20). After three washes with TNT buffer, nitrocellulose membranes were incubated with alkaline phosphatase conjugated secondary antibodies and revealed with 5-bromo-4-chloro-3-indolyl phosphate/nitro blue tetrazolium (BCIP/NBT; Promega).

Immunofluorescence microscopy. IFAs on intracellular parasites on HFFs cells were conducted as described previously²⁹. Note that RON labelling in the rhoptries have been performed after methanol fixation while RON labelling at the moving junction have been performed after formaldehyde 4% fixation, followed by 0, 1% saponin permeabilization. The antibodies used and their dilution for IFA are listed in Supplementary Table S2. Samples were observed with a Zeiss Axioimager epifluorescence microscope. Images were acquired with a Zeiss AxioCam MRm CCD camera driven at the 'Montpellier resources imagerie' facility and processed using Zeiss Zen software. Adjustments for brightness and contrast were applied uniformly on the entire image.

Transfection and selection of transformants. 20×10^6 *T. gondii* tachyzoites were transfected by electroporation at 2.02 kV, 50 Ω and 25 μ F using an Electro Cell Manipulator 630 (BTX) with 30 μ g of plasmid DNA as described previously³⁰. 30 μ g of CRISPR/Cas9 plasmids plus 5 μ g of PCR products using the KOD polymerase were used to transfect parasites. Transgenic parasites were selected by addition of pyrimethamine at 2 μ M for pLIC-RON_{4L1} and pKO-RON_{4L1} vectors, and 30 μ g/ml of phleomycin for complementation. For N-terminal tagging of RON_{4L1}, parasites transiently expressing cas9-YFP-fluorescence were sorted by FACS two days after transfection and cloned into a 96-well plate for each transfection, clones were isolated by limiting dilution cloning and screened by PCR for correct DNA integration.

Plaque assays and invasion assays. Plaque assays and invasion assays were performed as described previously³¹. Independent invasion assays were performed three times in which at least 20 fields were quantified per coverslip (n = 3).

Co-immunoprecipitation. Parasites were solubilized in lysis buffer (1% NP40, 50 mM Tris-HCL pH8, 150 mM NaCl, 4 mM EDTA and protease inhibitor) and immunosorption procedures were done using anti-HA antibodies as described previously¹². After overnight incubation of the lysate on beads, HA-beads are washed 5 times in wash buffer (50 mM Tris pH8, 1 M NaCl and 0.5%NP40). Elution from beads was performed during 5 min at 95 °C with SDS-PAGE sample buffer. Western blots were performed on the eluates using rabbit anti-RON2-3, rabbit anti-RON4, rat anti-RON5, rat anti-RON8, rabbit anti-AMA1 and rat anti-HA antibodies. The antibodies dilutions used for western blot are described in Supplementary Table S2.

Glass beads antibody loading. Loading of antibodies was performed using glass-beads as originally described³². Acid-washed 150–212 μ m glass beads (Sigma) were washed 3 times with distilled water. 0.1 mg of beads were then resuspended in 300 μ l of the appropriate medium containing commercial anti-HA antibodies (Covalab) diluted at 1/30. HFF cultures growing on coverslips in a 24 wells-plate were washed twice with Hanks' Balanced Salt Solution (HBSS) before the antibodies-beads solution was put into each well. The beads were rolled onto the coverslip by tilting the plate ~10 times, until evenly distributed over its surface. The coverslip was then

transferred to another well where it was washed 3 times with HBSS and returned to DMEM culture medium and allowed to recover at 37°C and 5% CO₂ for 30 minutes. Invasion assays were then carried out by allowing *T. gondii* tachyzoites to sediment on the HFF for 20 minutes at 4°C and subsequently warming them during 2.5 min at 37°C to trigger invasion. Invasion was stopped and cells were fixed by adding an excess volume of 4% PAF in HBSS. The extracellular portion of the tachyzoites was labelled with rabbit SAG1. Parasites and cells were then permeabilized with 0.1% saponin and incubated with secondary antibodies.

Survival *in vivo*. 100 tachyzoites freshly harvested from cell culture were inoculated by intra-peritoneal (i.p.) injection in 8–10 week-old female BALB/c mice (Jackson laboratories). Simultaneously to injection, parasites infectivity was evaluated by plaque assay. 7 days post-infection, seropositivity against *Toxoplasma* infection was tested. Survival experiments were done on groups of 5 mice per parasite cell line. Survival experiments were repeated independently twice. Mice survival was checked on a daily basis until their death, endpoint of all experiments. Data were represented as Kaplan and Meier plots using Prism software (Graphpad).

Statistical analysis. All results are presented as mean values SEM. For invasion and plaque assays, one representative experiment is shown and two-tailed t-test has been used to determine significance. For *in vivo* experiments, levels of significance were determined with the Logrank test using GraphPad.

Data availability. All relevant data are included in the paper or the Supplementary Information.

References

- Aikawa, M., Miller, L. H., Johnson, J. & Rabbege, J. Erythrocyte entry by malarial parasites. A moving junction between erythrocyte and parasite. *J Cell Biol* **77**, 72–82 (1978).
- Alexander, D. L., Mital, J., Ward, G. E., Bradley, P. & Boothroyd, J. C. Identification of the Moving Junction Complex of *Toxoplasma gondii*: A Collaboration between Distinct Secretory Organelles. *PLoS Pathog* **1**, e17 (2005).
- Lebrun, M. *et al.* The rhoptry neck protein RON4 relocalizes at the moving junction during *Toxoplasma gondii* invasion. *Cell Microbiol* **7**, 1823–1833 (2005).
- Besteiro, S., Michelin, A., Poncet, J., Dubremetz, J. F. & Lebrun, M. Export of a *Toxoplasma gondii* rhoptry neck protein complex at the host cell membrane to form the moving junction during invasion. *PLoS Pathog* **5**, e1000309 (2009).
- Straub, K. W., Cheng, S. J., Sohn, C. S. & Bradley, P. J. Novel components of the Apicomplexan moving junction reveal conserved and coccidia-restricted elements. *Cell Microbiol* **11**, 590–603 (2009).
- Dubremetz, J. F. Rhoptries are major players in *Toxoplasma gondii* invasion and host cell interaction. *Cell Microbiol* **9**, 841–848 (2007).
- Narum, D. L. & Thomas, A. W. Differential localization of full-length and processed forms of PF83/AMA-1 an apical membrane antigen of *Plasmodium falciparum* merozoites. *Mol Biochem Parasitol* **67**, 59–68 (1994).
- Lamarque, M. *et al.* The RON2-AMA1 interaction is a critical step in moving junction-dependent invasion by apicomplexan parasites. *PLoS Pathog* **7**, e1001276 (2011).
- Tyler, J. S. & Boothroyd, J. C. The C-terminus of *Toxoplasma* RON2 provides the crucial link between AMA1 and the host-associated invasion complex. *PLoS Pathog* **7**, e1001282, <https://doi.org/10.1371/journal.ppat.1001282> (2011).
- Tonkin, M. L. *et al.* Host cell invasion by apicomplexan parasites: insights from the co-structure of AMA1 with a RON2 peptide. *Science* **333**, 463–467 (2011).
- Vulliez-Le Normand, B. *et al.* Structural and functional insights into the malaria parasite moving junction complex. *PLoS pathogens* **8**, e1002755 (2012).
- Lamarque, M. H. *et al.* Plasticity and redundancy among AMA-RON pairs ensure host cell entry of *Toxoplasma* parasites. *Nat Commun* **5**, 4098, <https://doi.org/10.1038/ncomms5098> (2014).
- Guerin, A. *et al.* Efficient invasion by *Toxoplasma* depends on the subversion of host protein networks. *Nat Microbiol* **2**, 1358–1366, <https://doi.org/10.1038/s41564-017-0018-1> (2017).
- Wang, M. *et al.* The moving junction protein RON4, although not critical, facilitates host cell invasion and stabilizes MJ members. *Parasitology*, 1–8, <https://doi.org/10.1017/S0031182017000968> (2017).
- Straub, K. W., Peng, E. D., Hajagos, B. E., Tyler, J. S. & Bradley, P. J. The moving junction protein RON8 facilitates firm attachment and host cell invasion in *Toxoplasma gondii*. *PLoS Pathog* **7**, e1002007, <https://doi.org/10.1371/journal.ppat.1002007> (2011).
- Beck, J. R., Chen, A. L., Kim, E. W. & Bradley, P. J. RON5 is critical for organization and function of the *Toxoplasma* moving junction complex. *PLoS Pathog* **10**, e1004025, <https://doi.org/10.1371/journal.ppat.1004025> (2014).
- Bargieri, D. Y. *et al.* Apical membrane antigen 1 mediates apicomplexan parasite attachment but is dispensable for host cell invasion. *Nat Commun* **4**, 2552, <https://doi.org/10.1038/ncomms3552> (2013).
- Giovannini, D. *et al.* Independent roles of apical membrane antigen 1 and rhoptry neck proteins during host cell invasion by apicomplexa. *Cell Host Microbe* **10**, 591–602, <https://doi.org/10.1016/j.chom.2011.10.012> (2011).
- Parker, M. L. *et al.* Dissecting the interface between apicomplexan parasite and host cell: Insights from a divergent AMA-RON2 pair. *Proc Natl Acad Sci USA* **113**, 398–403, <https://doi.org/10.1073/pnas.1515898113> (2016).
- Boothroyd, J. C. & Dubremetz, J. F. Kiss and spit: the dual roles of *Toxoplasma* rhoptries. *Nat Rev Microbiol* **6**, 79–88 (2008).
- Behnke, M. S. *et al.* Coordinated progression through two subtranscriptomes underlies the tachyzoite cycle of *Toxoplasma gondii*. *PLoS One* **5**, e12354, <https://doi.org/10.1371/journal.pone.0012354> (2010).
- Fritz, H. M. *et al.* Transcriptomic analysis of toxoplasma development reveals many novel functions and structures specific to sporozoites and oocysts. *PLoS One* **7**, e29998, <https://doi.org/10.1371/journal.pone.0029998> (2012).
- Behnke, M. S., Zhang, T. P., Dubey, J. P. & Sibley, L. D. *Toxoplasma gondii* merozoite gene expression analysis with comparison to the life cycle discloses a unique expression state during enteric development. *BMC Genomics* **15**, 350, <https://doi.org/10.1186/1471-2164-15-350> (2014).
- Huynh, M. H. & Carruthers, V. B. Tagging of endogenous genes in a *Toxoplasma gondii* strain lacking Ku80. *Eukaryot Cell* **8**, 530–539 (2009).
- Carey, K. L., Jongco, A. M., Kim, K. & Ward, G. E. The *Toxoplasma gondii* rhoptry protein ROP4 is secreted into the parasitophorous vacuole and becomes phosphorylated in infected cells. *Eukaryot Cell* **3**, 1320–1330 (2004).
- Carruthers, V. B. & Sibley, L. D. Sequential protein secretion from three distinct organelles of *Toxoplasma gondii* accompanies invasion of human fibroblasts. *Eur J Cell Biol* **73**, 114–123 (1997).
- Poukchanski, A. *et al.* *Toxoplasma gondii* Sporozoites Invade Host Cells Using Two Novel Paralogues of RON2 and AMA1. *PLoS One* **8**, e70637 (2013).
- Frenal, K., Dubremetz, J. F., Lebrun, M. & Soldati-Favre, D. Gliding motility powers invasion and egress in Apicomplexa. *Nature Reviews* in press (2017).

29. El Hajj, H. *et al.* Molecular signals in the trafficking of *Toxoplasma gondii* protein MIC3 to the micronemes. *Eukaryot Cell* **7**, 1019–1028 (2008).
30. Kim, K., Soldati, D. & Boothroyd, J. C. Gene replacement in *Toxoplasma gondii* with chloramphenicol acetyltransferase as selectable marker. *Science* **262**, 911–914 (1993).
31. Daher, W. *et al.* Lipid kinases are essential for apicomplast homeostasis in *Toxoplasma gondii*. *Cell Microbiol* **17**, 559–578, <https://doi.org/10.1111/cmi.12383> (2015).
32. McNeil, P. L. & Warder, E. Glass beads load macromolecules into living cells. *J Cell Sci* **88**(Pt 5), 669–678 (1987).

Acknowledgements

We Thank Damien Jacot and the flow cytometry facility, CMU, Geneva for their work with sorting parasites. We thank Boris Striepen, Michael Cipriano and Sebastian Lourido for plasmids. This research was supported by the ANR (ANR-16-CE15-0010-01), Laboratoire d'Excellence (LabEx) (ParaFrap ANR-11-LABX-0024), by the Fondation pour la Recherche Médicale (Equipe FRM DEQ20130326508) to ML. A.G. has been supported by ParaFrap (ParaFrap ANR-11-LABX-0024) and is a recipient of FRM (award no. FDT20160435387). M.L. gratefully acknowledges the "Montpellier Ressources Imagerie" technical platform for access to their microscopes and cell sorters. ML and SB are INSERM researchers.

Author Contributions

A.G. and M.L. designed the study; A.G. performed all the study related to RON4_{T1} and its phenotypic characterization *in vitro*. A.G. and S.B. performed the topology analysis of RON4_{T1}. H.E.H. performed *in vivo* experiments. D.P.V. performed immuopurifications and immunofluorescences. A.G. and M.L. analysed the data and wrote the manuscript.

Additional Information

Supplementary information accompanies this paper at <https://doi.org/10.1038/s41598-017-18010-9>.

Competing Interests: The authors declare that they have no competing interests.

Publisher's note: Springer Nature remains neutral with regard to jurisdictional claims in published maps and institutional affiliations.



Open Access This article is licensed under a Creative Commons Attribution 4.0 International License, which permits use, sharing, adaptation, distribution and reproduction in any medium or format, as long as you give appropriate credit to the original author(s) and the source, provide a link to the Creative Commons license, and indicate if changes were made. The images or other third party material in this article are included in the article's Creative Commons license, unless indicated otherwise in a credit line to the material. If material is not included in the article's Creative Commons license and your intended use is not permitted by statutory regulation or exceeds the permitted use, you will need to obtain permission directly from the copyright holder. To view a copy of this license, visit <http://creativecommons.org/licenses/by/4.0/>.

© The Author(s) 2017